

# SYMPOSIUM 1988 TRONDHEIM



## A CHARACTERIZATION PROCEDURE FOR THE DYNAMIC BEHAVIOR OF FRANCIS TURBINES: PRACTICAL COMPARISON OF ELBOW AND MOODY TYPE DRAFT TUBES.

|             |                     |             |
|-------------|---------------------|-------------|
| JACOB T.    | IMHEF, EPF-Lausanne | Switzerland |
| PRÉNAT J.E. | IMHEF, EPF-Lausanne | Switzerland |
| GRENIER R.  | Dominion Eng. Works | Canada      |

### Synopsis

Characterization from model tests of the dynamic behavior of hydraulic turbines operating off design conditions is an important step in the knowledge of instability phenomena. IMHEF at EPF-Lausanne, Switzerland meets this purpose with a standard test procedure. Simple, fast and efficient, it yields complete and easily interpreted results. This test procedure is used here to compare the dynamic characteristics of elbow and Moody type draft tubes.

Relevant frequencies and cavitation compliance are expressed as functions of the machine flow rate. The runner design has a dominant influence on the occurrence of part-load resonance on the tested model. Modifications of dynamic phenomena by an internal structure of the draft tube are shown.

The need for generalization of such tests appears clearly from these results.

### Résumé

La caractérisation au stade des essais sur modèle réduit du comportement dynamique des turbines hydrauliques fonctionnant hors de leur régime nominal est une étape importante vers la connaissance des phénomènes d'instabilités. L'IMHEF à l'EPF-Lausanne (Suisse) propose à cet effet une procédure d'essai standard, rapide et simple à mettre en oeuvre, qui donne des résultats clairs et complets. Cette procédure permet ici d'établir une comparaison des comportements dynamiques d'aspirateurs coudé et de type Moody.

Les fréquences significatives et la coupeselle de cavitation sont exprimées en fonction du débit-volume de la machine. L'influence dominante du tracé de l'aubage sur les phénomènes de résonance à charge partielle est démontrée sur le modèle étudié. L'effet d'une structure interne de l'aspirateur est mis en évidence.

Ces résultats font clairement apparaître la nécessité de la généralisation de ce type d'essai.

F5

## 1. Introduction

An important part of the activities of the Hydraulic Machines and Fluid Mechanics Institute of EPF-Lausanne is the conduction of model tests for the development and verification of technical guarantees of hydraulic machines.

In the case of Francis turbines, the trend toward ever higher specific powers leads to stability problems. Technical requirements for hydraulic equipments now often include specifications on pressure swings in off design ranges. These particular operating conditions can't be fully described by state-of-the-art flow computations, so model tests are -and will be for some time- the only solution.

In this purpose, IMHEF sets up a fast and efficient test procedure for the qualification on small scale models of Francis turbines [3]. It yields a fairly good knowledge of dynamic characteristics of the studied model, and requires a relatively simple equipment and a moderate test time.

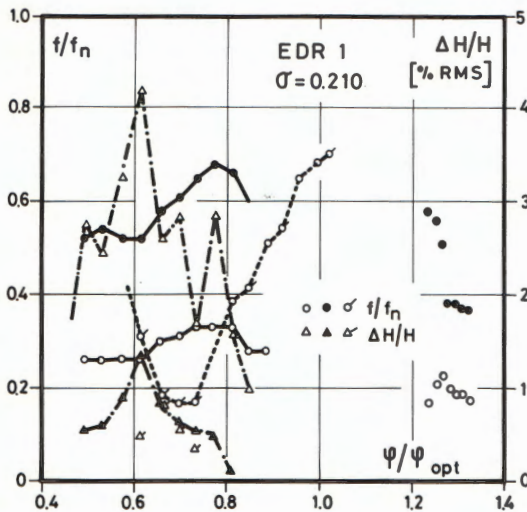
This standard test is mainly a survey of oscillations vs. gate opening (gradual opening of the wicket gate with constant test head, Thoma parameter  $\sigma$  and rotation speed at best efficiency specific energy  $\psi$ ) [8], followed by a detailed study of influences from  $\sigma$  and  $\psi$  for points of particular interest. Measured pressure and torque fluctuations are systematically analyzed using Fourier transform. Oscillations are surveyed for the prototype rated  $\sigma$ , and also for another  $\sigma$  value, obtained from statistical data [3], for a more general appreciation of encountered phenomena.

Relative frequencies of part-load fluctuations (rotating pressure field) and of part-load and full load free oscillations are obtained from this test. These relative frequencies are fairly well transposable from model to prototype. Amplitude levels may be surveyed. Conditions for the development of surges -full load pulsation and part load resonance- are observed. The cavitation compliance can also be derived from this test. All this information is available in the whole operating range.

As a practical example of this standard test procedure, a detailed study of a high specific speed Francis turbine model is put forward here, with different configurations of runners and draft tubes.

Results are published courtesy of Dominion Engineering Works, Canada, designer and owner of the turbine model.

## 2. Standard dynamic testing of a Francis turbine model



Basic phenomena and some terminology are first introduced from previously detailed results [3]: the study of a high specific speed Francis turbine model ( $nq=95$ ), with a 405mm diameter runner, at  $\sigma=0.210$  under a test head of 10mWC.

Figure 2 (EDR1) shows  $\Delta H/H$  as a function of relative flow rate  $\psi/\psi_{opt}$  an arrangement of amplitude / frequency spectra of the pressure read from a reference sensor (do co, fig.3), in the oscillations survey. Spectral analysis is performed from 0 to  $2f_n$ . A diagram in figure 1 highlights the main phenomena (peaks at  $f_n$  and  $2f_n$  are related to normal faults in the model runner rotation).

Figures 1&2: Pressure fluctuation relative frequencies and amplitudes at  $\psi_{opt}$ . Diagram for EDR1 ( $\uparrow$ ) and arrangement of spectra ( $\downarrow$ ) for EDR1 and EDR2 (two  $\sigma$  values)

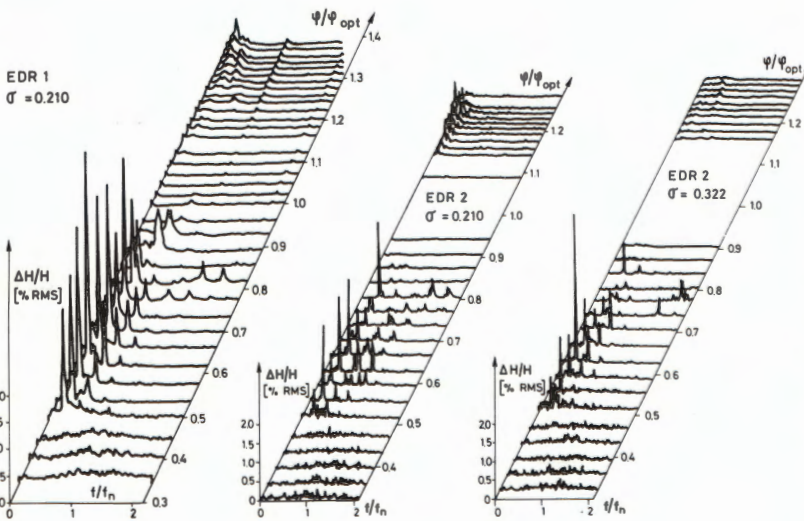


Figure 5 (EDR1) also gives for the part load range fluctuations picked up across the cone from the reference sensor (up co) and at the spiral case inlet (ca in).

**Part load ( $\psi/\psi_{opt} < 1$ )** mainly exhibits a rotating pressure field.

Its frequency is marked ( $\circ$ ). It is visualized by the motion of the typical helical cavitating vortex core.

The frequency of free oscillations in the draft tube ( $\sigma$ ) goes through a minimum at the flow rate for which the cavity volume is maximum. It rises roughly linearly with  $\sigma$  and with  $\psi$ .

The rotating pressure field frequency ( $\circ$ ) decreases from very small gate openings to part load, then stabilizes around  $\phi/\phi_{opt} = 0.5$ . Associated amplitudes are high. The frequency then grows slightly at  $0.6\phi_{opt}$  to fall again by  $0.8\phi_{opt}$ .

This local rise corresponds to the maximum of cavity volume, i.e. minimal free oscillation frequency. The fluctuation associated with the rotating pressure field is in phase opposition across the draft tube cone.

Frequencies of free oscillation and rotating pressure field have the same value for two relative flow-rates. This leads to an amplification of the rotating pressure field (fig 5). The phase difference between up co and do co then becomes significantly different from  $180^\circ$ .

The test head has no influence on the rotating pressure field relative frequency ( $\circ$ ). This frequency depends in the range  $0.6 < \phi/\phi_{opt} < 0.8$  on the cavity volume ( $f/f_n$  grows as the volume increases) but is otherwise independent of  $\sigma$ . The absolute frequency is not much altered by large changes in  $\psi$ .

The rotating pressure field 2nd harmonic frequency ( $\bullet$ ) goes through the same evolution, with smaller amplitudes. This fluctuation is in phase between up co and do co.

A group of peaks, is visible near  $2f_n$  at about  $0.8\phi_{opt}$ . This phenomenon induces remarkable model vibrations and may be the one mentioned in [8] as occurring "on all tested models and the prototype". It is disorganised only by the long cone pile (MDLC, see 5.).

**Full load** ( $\phi/\phi_{opt} > 1$ ) exhibits the free oscillations extensively described in [1,2 and 8], leading to pulsation for extreme gate openings.

➔ Proceeding from the knowledge of these phenomena for one configuration, the standard test procedure for the characterization of the dynamic behavior of Francis turbines allows a proper perception of changes due to modifications of the runner and draft tube.

| Test | Runner              | Draft tube             |
|------|---------------------|------------------------|
| EDR1 | original, $nq=95$   | elbow type             |
| EDR2 | modified*, $nq=100$ | elbow type             |
| MDSC | modified*, $nq=100$ | Moody type, short cone |
| MDLC | modified*, $nq=100$ | Moody type, long cone  |

\* modification: 11% increase in optimal flow-rate

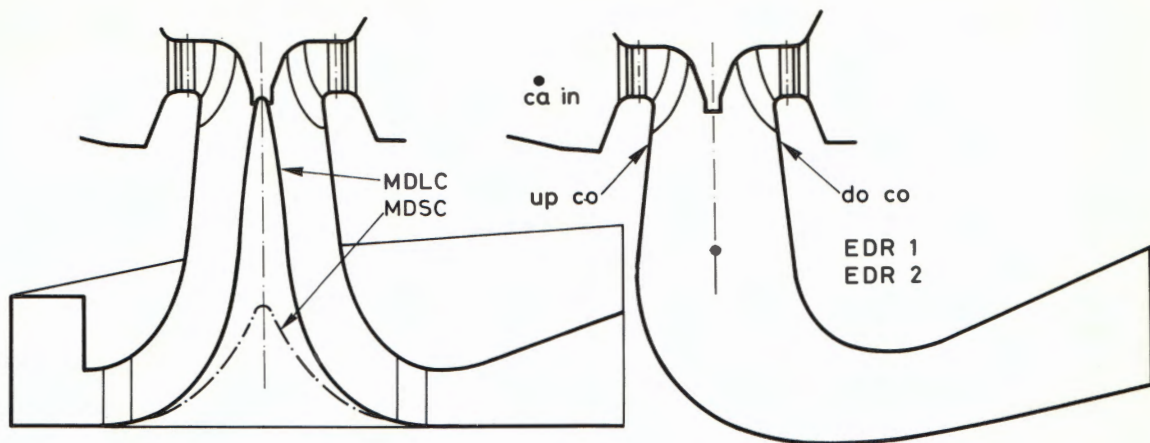


Figure 3: Elbow and Moody type draft tubes

### 3. Changing from runner 1 to runner 2 in the elbow type draft tube

Results of the survey of oscillations for elbow type draft tube, runner 2 (EDR2) at  $\sigma=0.210$  are shown in figures 2 and 4. Similarities with case EDR1 in the development of basic phenomena are evident.

The evolution of fluctuations is shifted to smaller values of  $\phi/\phi_{opt}$  as we change from EDR1 to EDR2.

This, like the global rise in the frequency of the rotating pressure field, is due to the difference in geometry. It is worth noting that the relative frequency increased for a higher specific speed. This goes against the conventional trend [7].

As we change from  $\sigma=0.210$  to  $\sigma=0.322$  (EDR2), the frequency of free oscillation clearly increases. This is noteworthy since at  $\sigma=0.322$ , the rotating pressure field no longer excites the draft tube at its resonating frequency. This is an important element in the general appreciation of the dynamic behavior of a Francis turbine.

The free oscillation frequency reaches a higher value for EDR2. This difference is connected to velocities distribution at runner exit, which determines the cavity volume in the helical vortex, and was not optimized in EDR1. Regarding part load resonance problems, modifications in the runner design resulted in a lower acceptable value for plant  $\sigma$ .

The local rise in rotating pressure field frequency is attenuated in the EDR2 test at  $\sigma=0.322$ . This may be expected, as the cavity volume, which apparently causes this local frequency rise, is smaller when  $\sigma$  increases.

Full load phenomena at  $\sigma=0.322$  have greater frequencies and lower amplitudes than at  $\sigma=0.210$ . This agrees with previously established trends [1,2].

Figures 4 and 5 (obtained from two different readings) exhibit differences in amplitude with identical frequencies. This was commented in [3]; it shows how misleading may be an interpretation of amplitudes picked up on a single sensor in the draft tube.

→ Testing two runners in the same draft tube, we observe the same basic dynamic phenomena. Comparison of the results highlights each runner's particular properties. The possible influence of runner design on the acceptable  $\sigma$  value for part load resonance is demonstrated.

#### **4. Elbow type and Moody (short cone) type draft tubes**

In renewing existing power plants, one may be brought to fit a modern runner in a draft tube of ancient design. It is then interesting to evaluate from model tests the behavior of such compounds. The elbow type draft tube (EDR2) is compared with a Moody type draft tube with a short cone central pile (MDSC) and then with a long cone (MDLC, see figure 3).

The rotating pressure field frequency and its 2nd harmonic are the same for tests EDR2 and MDSC, even in the range of local frequency rise. Runner and draft tube cone are identical; it is then easy to admit that the elbow shape might play a negligible role in these fluctuations.

Free oscillations occur at the same frequency in the two draft tubes, for both  $\sigma$  values, except in a small range of  $\phi/\phi_{opt}$  around 0.55 at  $\sigma=0.210$ .

Amplitudes are grossly comparable between MDSC and EDR2 (figure 5).

→ A comparative test of elbow type and Moody type (with short conical pile) draft tubes shows no significant modification of the dynamic behavior.

#### **5. Moody type draft tube with short and long cone**

MDLC tests feature a new oscillation ( $\varphi$ , fig 4), around  $0.6f_n$  ( $\sigma=0.210$ ) or  $0.5f_n$  ( $\sigma=0.322$ ) at  $0.75\phi_{opt}$ . Variable in frequency according to  $\phi$  and  $\sigma$ , low in amplitude and in phase opposition across the draft tube, it does not appear in other configurations.

Part load phenomena otherwise develop in the same way. A clear shift in flow rate of frequency evolutions may be observed.  $\phi/\phi_{opt}=0.5$  for MDLC corresponds to  $\phi/\phi_{opt}=0.55$  with the short cone central pile.

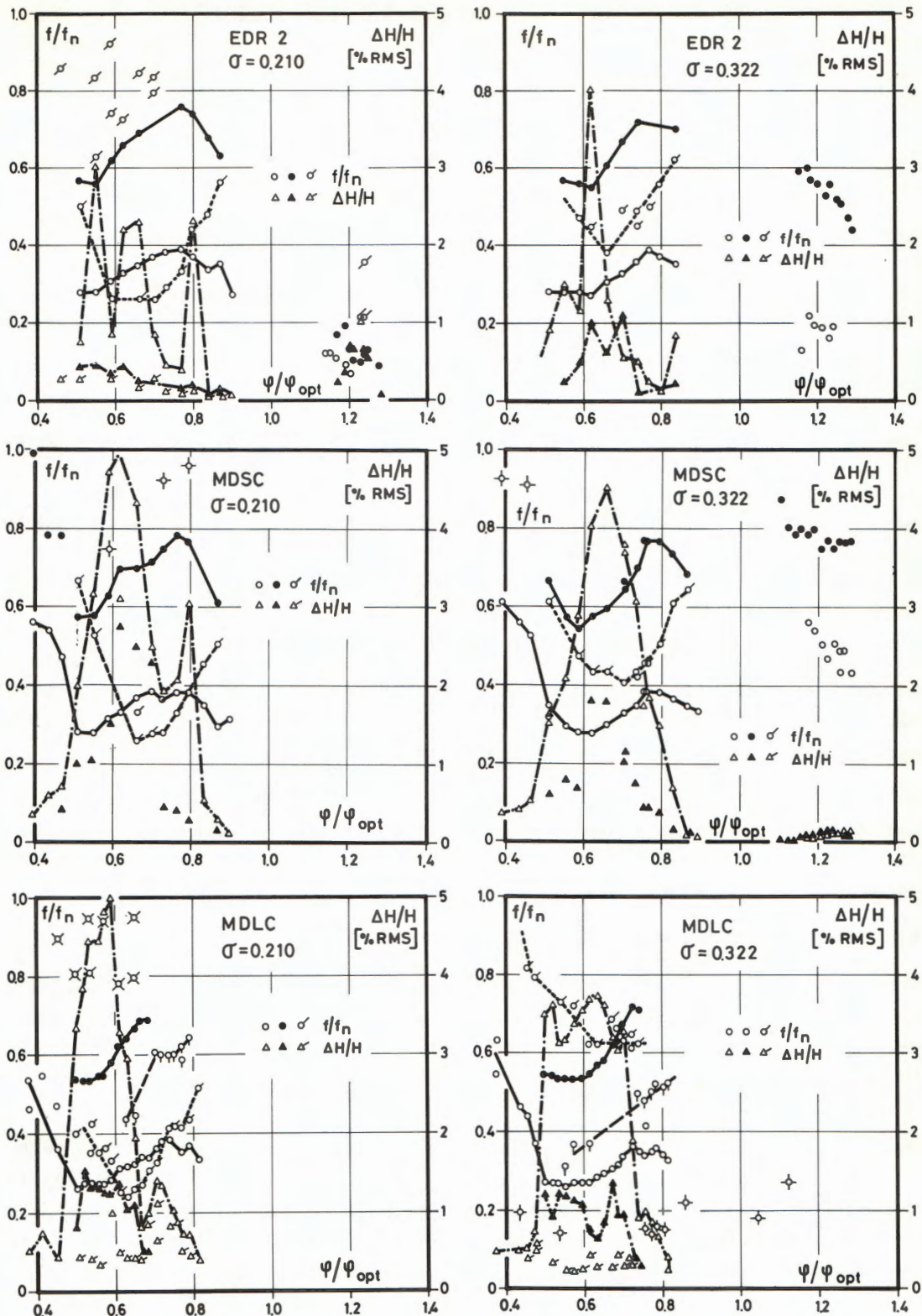


Figure 4: Survey of oscillations for EDR2, MDSC and MDLC

A slight difference in the rotating pressure field frequency can be seen in the local rise range. It is more evident on the 2nd harmonic and greater at  $\sigma=0.210$  than at  $\sigma=0.322$ . This local rise in frequency has already been linked to modifications of velocities distribution at runner exit. The introduction of a structure within the draft tube cone will in this way affect the rotating pressure field frequency.

Aside from the shift in  $\phi/\phi_{opt}$ , the frequency of free oscillations is the same for MDSC and MDLC at  $\sigma=0.210$ . At  $\sigma=0.322$ , it is 50% higher for MDLC. A detailed investigation of  $\sigma$  variations at part load shows that this frequency grows linearly with  $\sigma$ , but with a slope greater for MDLC than for MDSC. For the two configurations, free oscillation frequencies are comparable at  $\sigma=0.210$ .

Full load phenomena disappear completely with the MDLC. We know that these are free oscillations [2]. On this machine, the full load cavity is axial with a small diameter [3]. It results from the runner exit swirl, which in this direction (opposite from the runner's) forms a stable vortex line. A structure occupying the draft tube centerline will result in a limitation of the circumferential velocity and will thus prevent cavity formation.

On the spectra arrangement in figure 2, a group of amplitude peaks can be seen near  $2f_n$  at  $\phi/\phi_{opt}=0.8$ . Their frequency is strongly dependant of  $\phi$  with a constant  $\sigma$  and of  $\sigma$  with a constant  $\phi$ . These fluctuations appear in all configurations except MDLC.

➔ Finally, the short cone pile is compared to the long cone inside the Moody type draft tube. This structure alters velocities distribution in the cavity vicinity and in this way modifies pressure fluctuations. It suppresses full load oscillations.

## 6. Identification of cavitation compliance

Stability computations on hydraulic power plants require a preliminary knowledge of the cavitation compliance. This problem has led to some extensive studies some years ago in the case of propellant feed pumps for launch vehicles. For Francis turbines, available results are scarce, although the need for such results is widely accepted [4].

The cavitation compliance is  $C \cdot H = -(\partial V_{ol}/\partial \sigma)$ , where  $V_{ol}$  is the cavity volume in the runner exit flow and  $H$  is the test head.  $C$  is schematically a lumped capacitance. The corresponding non-dimensional number is  $C^* = C \cdot H/R^3 = -(\partial V_{ol}/\partial \sigma)/R^3$ . In a previous paper [1], we evaluated  $C$  from observations of cavity volumes with variations of  $\sigma$ .



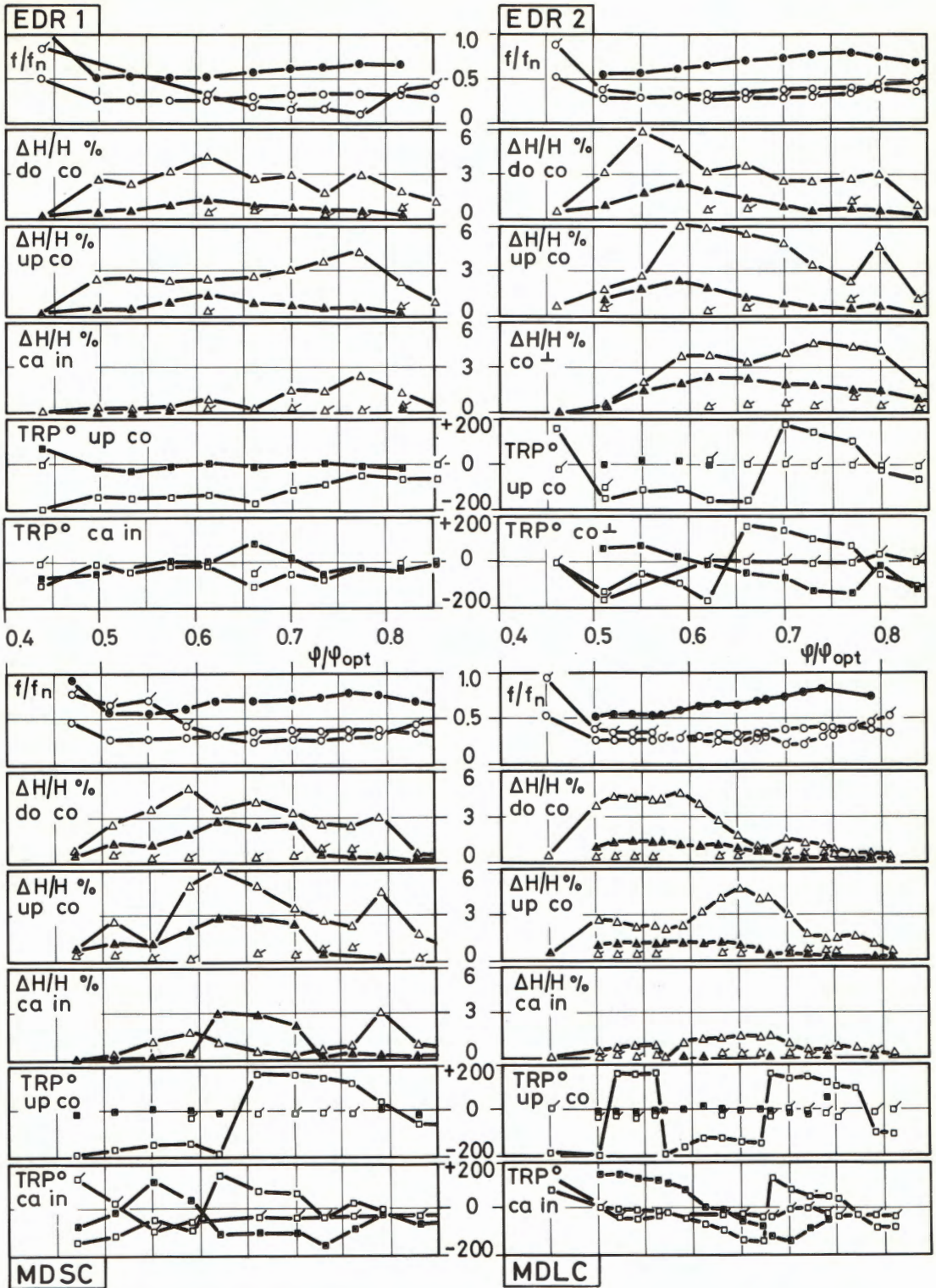


Figure 5: Detailed study of the part-load range

The non-dimensional cavitation compliance  $C^*$  may be transposed from model to prototype, with respect to some similitude laws. Mainly, the reference level for  $\sigma$  must be chosen so as to be representative of static pressures near the vortex core cavity. This problem of  $\sigma$  reference level could by itself be the subject for a most interesting investigation. A by-pass solution is to make model tests under Froude's head.

In an isothermic, perfect gas approximation, neglecting mass transfers, the cavitation compliance  $-\partial Vol/\partial \sigma$  is equal to the cavity volume. This gross approximation gives an idea of the order of magnitude of this important parameter.

The flow in the draft tube is reduced to an elementary oscillator, consisting of an inertia  $L$  connected to a lumped capacitance  $C$  at one end and to a free water level at the other end. The free oscillation frequency is then a function of  $C$  and  $L$ . This approximation does not consider the distributed compliance of the fluid within the draft tube. It accounts only for the first oscillatory mode.

Practically,  $C$  may be derived from the frequency of free oscillations. However, this quick method has some drawbacks. First of all, the inertia of the fluid column must be expressed. This can be obtained by integration of the draft tube geometry for the elbow type, but is quite uneasy for the Moody type.

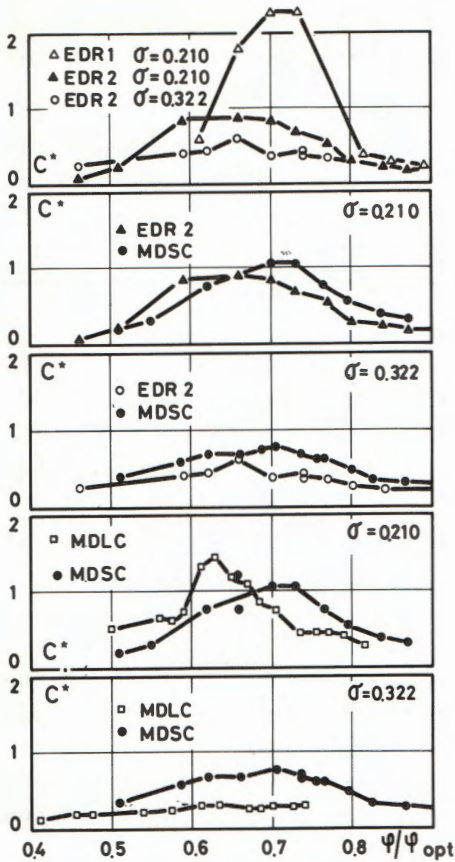
Then, the evolution of the free oscillation frequency must be precisely known. It is plagued with some scattering due to analysis resolution, to low amplitudes and -last but not least- to dynamic fluctuations of  $C$ . Finally, a reasonable value for the error on  $C^*$  would be  $\pm 15\%$  in the tests presented here. Although not quite satisfactory, this improves the precision of cavitation simulation in current stability computations.

## 7. Comparison of non-dimensional cavitation compliances $C^*$

Figure 6 gives the non-dimensional cavitation compliance as a function of  $\phi/\phi_{opt}$  at part load for EDR1 ( $\sigma=0.210$ ) and EDR2 ( $\sigma=0.210$  and  $0.322$ ).  $C^*$  goes through a maximum for  $\phi/\phi_{opt}$  values corresponding to a big cavity in the helical vortex core.  $C^*$  values are distinctly smaller at  $\sigma=0.322$  than at  $\sigma=0.210$ . Curve EDR2 is shifted in  $\phi/\phi_{opt}$ , compared with EDR1, as seen in (3.).

A small change in runner design can greatly affect the cavitation compliance. We can already say that it will be very difficult to evaluate this parameter from statistical data.

← Figure 6: Cavitation compliance



Comparison of MDSC with MDLC shows that the alteration of  $C^*$  due to the long cone is much smaller than that due to runner modification. We find again the shift in  $\phi/\phi_{opt}$  mentioned in (5.). Reduction of the cavity volume as we change from  $\sigma=0.210$  to  $\sigma=0.322$  is also quite remarkable.

The evolution of  $C^*$  is also given in the range  $0.4 < \phi/\phi_{opt} < 0.9$  for EDR2 and MDSC,  $\sigma=0.210$  and  $0.322$ . The maximum of  $C^*$  is slightly higher and shifted to superior flow rates in the Moody type draft tube.

### 8. Conclusions

Testing two runners in the same draft tube, we observe the same basic dynamic phenomena. Comparison of the results highlights each runner's particular properties. The possible influence of runner design on the acceptable  $\sigma$  value for part load resonance is demonstrated.

A comparative test of elbow type and Moody type (with short conical pile) draft tubes shows that the dynamic behavior is not affected by a change in the evolution of sections in the draft tube elbow.

The short cone pile is compared to the long cone inside the Moody type draft tube. This structure alters velocities distribution in the cavity vicinity and in this way modifies pressure fluctuations. It suppresses full load oscillations.

The method proposed for the quick determination of cavitation compliance is very easy to operate. Its precision does not give full satisfaction. However, the compliance suffers important dynamic variations, and the error in this determination is much smaller than currently admitted in stability computations. This contribution provides an improved solution for the evaluation of this important parameter.

Introduction of a central cone in the Moody type draft tube has only a small influence on  $C^*$ , whereas a change in runner design has a considerable importance.

This sensibility of  $C^*$  to small differences in runner exit velocity field forecasts great difficulties in the establishment of general laws. For the moment, it is important to compile a large number of test results on different machines, to grasp a clear image of the problem.

Finally, the easy interpretation of phenomena obtained through the standard test procedure is a striking demonstration of its efficiency. Fast and simple in execution, it should in the future be a part of all model tests arrangements.

---

### Sources

- [1] PRENAT J.-E., JACOB T.: Comportement à forte charge d'un modèle de turbine Francis et effets d'échelle. AIRH Symposium Montréal (1986)
- [2] JACOB T., MARIA D., PRENAT J.-E.: Comportement dynamique d'une turbine Francis à forte charge. Comparaisons modèle - prototype. SHF Comité technique 134, Paris (1987)
- [3] JACOB T., PRENAT J.-E.: General study, on small scale models, of the dynamic behavior of Francis turbines. IAHR W.G. Lille (1987)
- [4] PULPITEL L.: Dynamic problems of a hydraulic system with a hydraulic machine. IAHR W.G. Lille (1987)
- [5] MUCIACCIA F., ROSSI G.: Experimental approach to the study of the dynamic behavior of a Francis turbine model at high specific speed when operating at reduced load. IAHR, WG. Mexico (1985)
- [6] ANGELICO G., MUCIACCIA F., ROSSI G.: Part load behavior of a turbine: a study on a complete model of hydraulic power plant. IAHR Symposium Montréal (1986)
- [7] DOERFLER P.: System dynamics of the Francis turbine half load surge. IAHR Symposium Amsterdam (1982)
- [8] FISHER R.K., PALDE U., ULITH P.: Comparison of draft tube surging of homologous scale models and prototype Francis turbines. IAHR Symposium Tokyo (1980)

---

|                    |   |            |  |
|--------------------|---|------------|--|
| $\phi$             | $\frac{\dot{V}}{\pi R^3 N}$ : specific flow-rate      | $\psi$     | $\frac{2gH}{(RN)^2}$ : specific energy |
| R                  | runner radius, m                                      | $\dot{V}$  | flow-rate, m <sup>3</sup> /s           |
| H                  | test head, mWC  | N          | rotation speed, rad/s                  |
| g                  | gravity ( $g=9.806 \text{ s/m}^2$ )                   | $\Delta H$ | pressure amplitude, mWC                |
| f                  | frequency, Hz   | $f_n$      | rotation frequency, Hz                 |
| $\text{Trp}^\circ$ | transfer function phase                               | opt        | denotes best efficiency                |
| Vol                | cavity volume, m <sup>3</sup>                         | $C^*$      | non-dimensional cavitation compliance  |
| $nq$               | $\frac{60fn\sqrt{\dot{V}}}{H^{3/4}}$ : specific speed | $\sigma$   | NPSH/H: cavitation parameter           |